

Observation of higher-order infrared modes in solid C₆₀ films

K.-A. Wang, A. M. Rao, and P. C. Eklund

Department of Physics & Astronomy and Center for Applied Energy Research, University of Kentucky, Lexington, Kentucky 40506

M. S. Dresselhaus

*Department of Electrical Engineering & Computer Science and Department of Physics,
Massachusetts Institute of Technology, Cambridge, Massachusetts 02139*

G. Dresselhaus

Francis Bitter National Magnet Laboratory, Massachusetts Institute of Technology, Cambridge, Massachusetts 02139

(Received 1 June 1993)

In this paper, we present a rich (4 strong F_{1u} first-order and an additional 98 weak lines) ir spectrum for a 4- μm -thick C₆₀ film on KBr in the range 400–4000 cm^{-1} . Most of the weak lines are identified with second-order combination modes. More accurate frequencies of some optically inactive modes in C₆₀ have been obtained by simultaneously analyzing the higher-order ir and Raman spectra. Isotope-induced symmetry lowering in C₆₀ molecules has also been observed and is responsible for activating several fundamental modes which would otherwise be ir inactive.

Solid C₆₀ is a nearly ideal molecular solid with ten ($2A_g + 8H_g$) Raman-active and four (F_{1u}) ir-active modes,^{1,2} consistent with group-theoretical predictions for an isolated C₆₀ molecule with icosahedral (I_h) symmetry.^{1,3} Out of the 174 ($=180-6$) intramolecular vibrational modes in an icosahedral C₆₀ molecule, only 46 distinct mode frequencies are possible.^{1,3} Some of these modes have been determined experimentally by first-order Raman and infrared (ir) spectroscopy,^{1,2,4} high-resolution electron-energy-loss spectroscopy (HREELS),⁵ photoluminescence (PL),⁶ and neutron inelastic-scattering (NIS) experiments.⁷ Of these various methods, the Raman and ir spectroscopies provide detailed information about mode symmetries, and the inherent high resolution affords a more accurate determination of the mode frequencies. Recently, we reported the observation and interpretation of numerous higher-order Raman features in solid C₆₀ at temperatures well above and below the orientational ordering transition.⁸ This prior Raman study in solid C₆₀ led us to conclude that most of the additional sharp features observed below 1600 cm^{-1} should be assigned to higher-order intramolecular scattering or to the isotopic activation of otherwise silent intramolecular modes,⁸ rather than to first-order scattering from otherwise Raman-silent modes activated by solid-state crystal-field effects.⁹ Consistent with the ir spectrum reported here, the sharpness of the observed second-order Raman features⁸ was taken as further important evidence that phonon dispersion in the solid state is very weak, supporting the picture of the nearly ideal molecular nature of solid C₆₀.

In this paper we report the observation of numerous higher-order sharp features in the ir spectrum of a thin film of solid C₆₀. Beside the four first-order-allowed (F_{1u}) ir modes, at least 98 additional weak lines are observed in the 400–4000 cm^{-1} frequency range, many of which are

tentatively identified with second-order combination modes, as discussed in greater detail below. Meanwhile, several of the weak lines are identified with first-order modes which would *not* be ir active in an isotopically pure C₆₀ molecule, but are proposed here to be activated by the isotopic substitution of naturally abundant ¹³C. From an analysis of the data, we are able to obtain values for many silent mode frequencies, which are found to be in good agreement with those obtained previously from analysis of the higher-order Raman spectrum.⁸ In addition to the four F_{1u} modes, Chase, Herron, and Holler¹⁰ also reported numerous other weak features in their ir spectrum for a thick ($d=14\ \mu\text{m}$) solid C₆₀ film. Although they discussed combination modes as a possible origin of the many weak lines in the spectrum, they did not make any specific assignments.

High-purity (99.7%) microcrystalline C₆₀ powder was first loaded into a quartz tube and degassed at 250°C under a dynamic vacuum 3×10^{-5} Torr for ~ 6 h in order to remove any residual solvent (mostly toluene). Details for the extraction and purification of C₆₀ can be found in our previous publications.¹ The heat-treated powder was then transferred into a molybdenum boat inside a film deposition chamber that is housed inside a glove box (helium atmosphere; O₂, H₂O < 1 ppm). *In situ* preheating the C₆₀ powder for ~ 15 min. was further carried out to minimize the amount of toluene impurity in the films. A sufficiently thick ($d \approx 4\ \mu\text{m}$) C₆₀ film was deposited onto a KBr substrate (1.0-in. diam, $\frac{1}{8}$ -in. thickness) in order to discern the weak higher-order and other spectral features in the ir transmission spectrum of solid C₆₀. The $T=300$ K transmission spectrum was recorded with 1 cm^{-1} resolution in a nitrogen purged Digilab FTS 80 Fourier-transform spectrometer equipped with a germanium-coated KBr beamsplitter and a triglycine sulfate (TGS) detector.

Figure 1(a) shows the near-normal incidence, room-temperature ir transmission spectrum for the C_{60} film on KBr in the frequency range $400\text{--}4000\text{ cm}^{-1}$. Figures 1(b) and 1(c) show, accordingly, the lower- and higher-

frequency portions of the same spectrum on an expanded scale to allow better observation of the weak sharp features. Narrow structures associated with various first- and higher-order vibrational modes are superimposed on

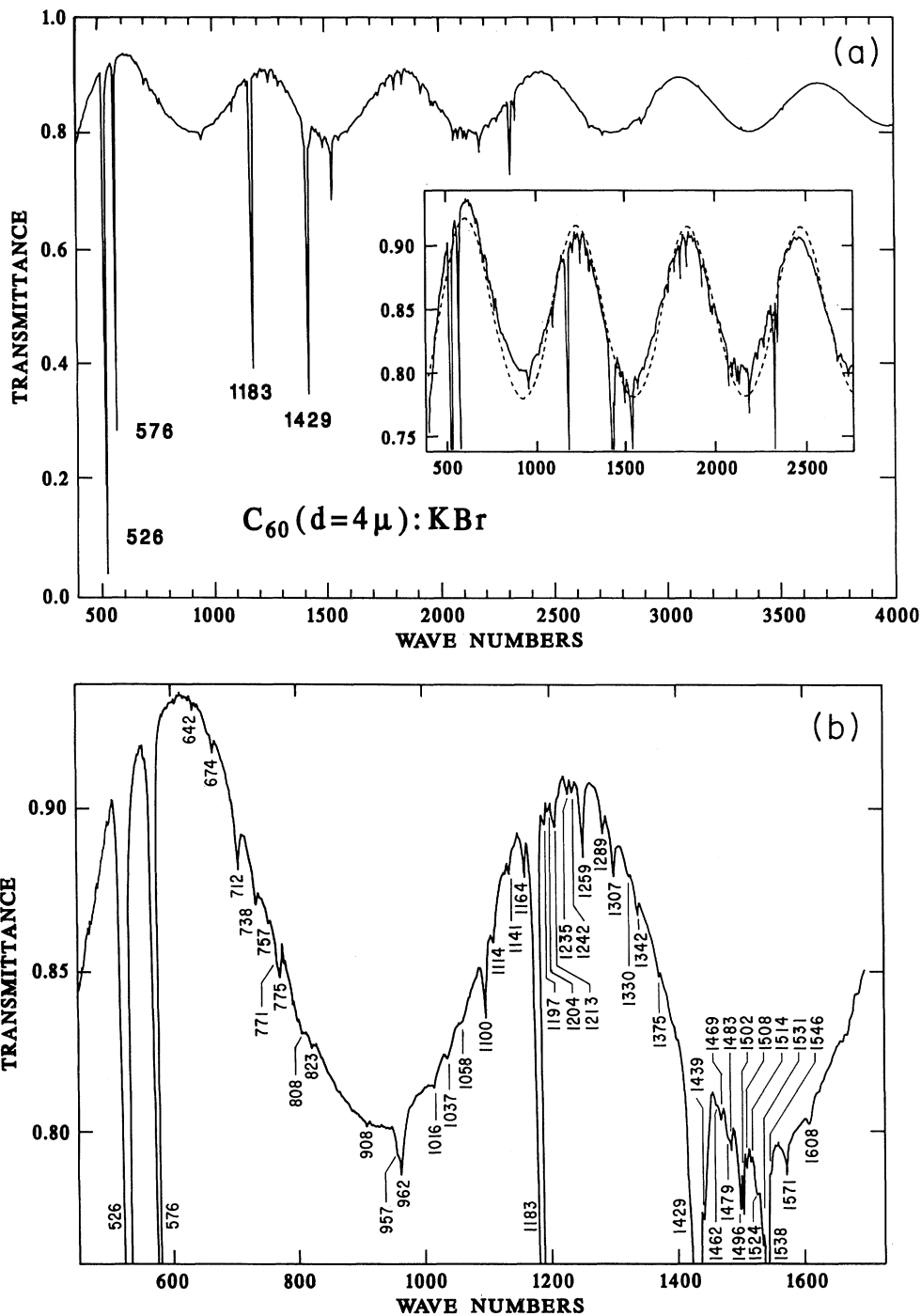


FIG. 1. (a) Infrared transmission ($400\text{--}4000\text{ cm}^{-1}$) spectrum ($T=300\text{ K}$) of a C_{60} film vacuum deposited on a KBr substrate. The four fundamental F_{1u} mode frequencies are indicated, and the large periodic oscillations are due to a Fabry-Perot interference effect in the C_{60} film. The inset shows a fit (dashed line) to the first four interference fringes using a model calculation (see text). (b) Low-frequency portion ($450\text{--}1700\text{ cm}^{-1}$) of (a). The experimentally determined ir frequencies are tabulated in Table II and are compared with theoretical predictions. (c) Same as in (b) for the high-frequency portion ($1700\text{--}3000\text{ cm}^{-1}$) of the figure.

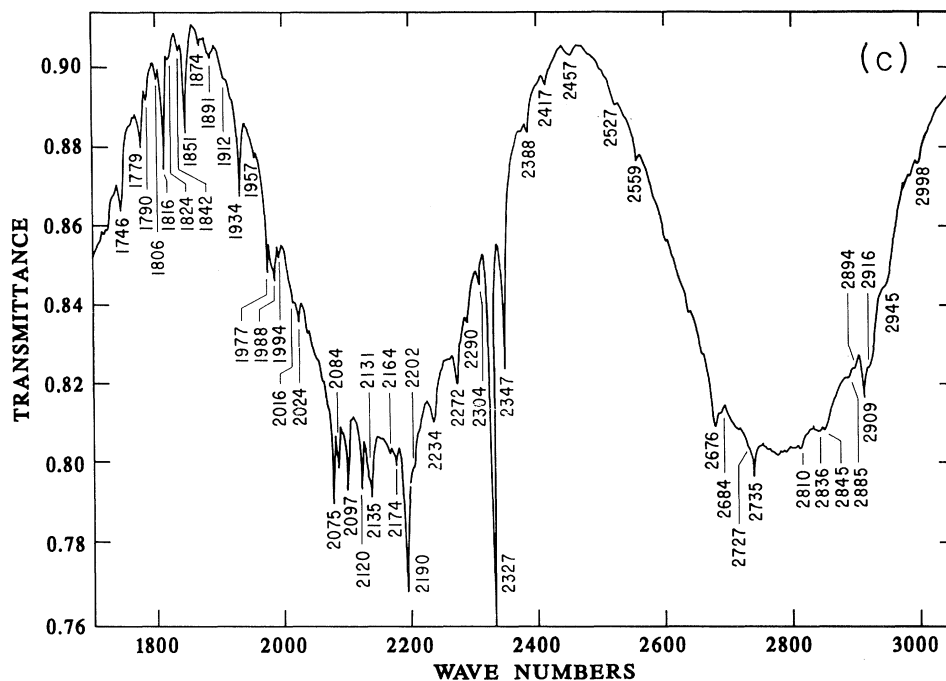


FIG. 1. (Continued).

a background exhibiting broad ($\sim 500\text{-cm}^{-1}$ period), large amplitude oscillations. These oscillations are due to an interference between the beams suffering various multiple internal reflections inside the C_{60} film (Fabry-Perot fringes). The inset to Fig. 1(a) shows a fit (dashed line) of the standard functional form for these fringes to data from a film of unknown thickness and refractive index on a KBr substrate ($n=1.5$). Fitting the first four fringes in the spectrum of Fig. 1(a), we have obtained a film thickness $d=4.1\ \mu\text{m}$ (close to that determined directly by the film thickness monitor) and a value for the core dielectric constant $\epsilon_{\text{core}}=3.9$, which is the electronic contribution to the static dielectric function. This latter result is in good agreement with the value $\epsilon_{\text{core}}=4.0\pm 0.05$, also obtained previously from interference fringes in the ir spectrum,¹¹ and may be compared to $\epsilon_{\text{core}}=4.4\pm 0.2$ deduced by low-frequency capacitance studies.¹² Whereas isolated molecules generally exhibit narrow first- and second-order ir and Raman features, most crystalline solids show only narrow first-order vibrational features ($k=0$ selection rule) and very broad second-order features (due to phonon dispersion). Therefore, the numerous, well-resolved, higher-order ir lines seen in Fig. 1 are taken as further independent evidence for the weak intermolecular interactions in solid C_{60} . Thus the vibrational properties of an isolated C_{60} molecule should explain well the intramolecular vibrational modes in solid C_{60} .

From group-theoretical arguments, the expected number of second-order lines in the ir spectrum of an isolated C_{60} molecule should be very large [a total of 384 ($\nu_i + \nu_j$) combination modes]. Since ir-active modes have odd parity, no overtone modes are expected in the second-order ir spectrum for C_{60} . The total number of combination modes can be found by counting the number of times the

symmetry F_{1u} is contained in the direct product $n_i\Gamma_i \otimes n_j\Gamma_j$, where Γ_i (or Γ_j) denotes the symmetry of one of the irreducible representations of the I_h group, and n_i (or n_j) is the number of vibrational modes with symmetry Γ_i (or Γ_j). The 46 distinct mode frequencies for a C_{60} molecule which were previously used for the low-temperature analysis of the higher-order Raman spectra⁸ are tabulated as Table I. The direct products $\Gamma_i \otimes \Gamma_j$ which characterize the second-order combination modes can be calculated by using the character table for the I_h group.^{1,3} For example, the direct product $F_{1g} \otimes F_{1u} = A_u + F_{1u} + H_u$ contains F_{1u} once, which indicates that an ir-active combination mode exists in the second-order ir spectrum arising from the F_{1u} and F_{1g} vibrations. Not all mode combinations yield F_{1u} symmetry in the direct product. For instance, H_g and F_{1u} modes do not result in ir-active combination modes in the second-order spectrum since $G_g \otimes F_{1u} = F_{2u} + G_u + H_u$ does not contain F_{1u} .

In principle, the second-order ir spectrum, just like the second-order Raman spectrum,⁸ could provide a method for determining the frequencies of optically silent vibrational modes (A_u , F_{1g} , F_{2g} , F_{2u} , G_g , G_u , and H_u). The observation of some of the higher-order ir lines in Fig. 1 suggests, on the basis of the group-theoretical arguments given above, that certain modes Γ_i which are silent in the first-order ir or Raman processes may participate in the higher-order ir spectrum. By making small adjustments in the frequencies of the silent modes, and using the accepted experimental frequencies for the A_g , H_g , and F_{1u} modes,¹ we have been able to assign most of the observed lines to second-order combination modes (Table II). The silent mode frequencies (denoted by "b" in Table I) have

TABLE I. Experimentally determined mode frequencies for the fundamental vibrations in an isolated C_{60} molecule. First-order ir- and Raman-active modes have F_{1u} and (A_g, H_g) symmetries, respectively. The frequencies of the optically silent modes ($A_u, F_{1g}, F_{2g}, F_{2u}, G_g, G_u,$ and H_u) marked with "b" have been adjusted to obtain the best overall agreement between the experimental and calculated second-order Raman and ir spectra. The superscript "i" denotes ir line frequencies identified with ^{13}C isotope-activated modes.

Even parity		Odd parity	
$\nu_i(R)$	Frequency (cm^{-1})	$\nu_i(R)$	Frequency (cm^{-1})
$\nu_1(A_g)$	497.5	$\nu_1(A_u)$	1143.0 ⁱ
$\nu_2(A_g)$	1470.0 ⁱ	$\nu_1(F_{1u})$	526.5
$\nu_1(F_{1g})$	502.0 ^b	$\nu_2(F_{1u})$	575.8
$\nu_2(F_{1g})$	975.5 ^b	$\nu_3(F_{1u})$	1182.9
$\nu_3(F_{1g})$	1357.5 ^b	$\nu_4(F_{1u})$	1429.2
$\nu_1(F_{2g})$	566.5 ^b	$\nu_1(F_{2u})$	355.5 ^b
$\nu_2(F_{2g})$	865.0	$\nu_2(F_{2u})$	680.0
$\nu_3(F_{2g})$	914.0	$\nu_3(F_{2u})$	1026.0 ^b
$\nu_4(F_{2g})$	1360.0	$\nu_4(F_{2u})$	1201.0 ^b
$\nu_1(G_g)$	486.0 ^b	$\nu_5(F_{2u})$	1576.5 ^b
$\nu_2(G_g)$	621.0	$\nu_1(G_u)$	399.5 ^b
$\nu_3(G_g)$	806.0	$\nu_2(G_u)$	760.0 ⁱ
$\nu_4(G_g)$	1075.5 ^b	$\nu_3(G_u)$	924.0 ^b
$\nu_5(G_g)$	1356.0 ^b	$\nu_4(G_u)$	970.0
$\nu_6(G_g)$	1524.5 ^{b,i}	$\nu_5(G_u)$	1310.0
$\nu_1(H_g)$	273.0	$\nu_6(G_u)$	1446.0 ^b
$\nu_2(H_g)$	432.5	$\nu_1(H_u)$	342.5 ^b
$\nu_3(H_g)$	711.0 ⁱ	$\nu_2(H_u)$	563.0 ^b
$\nu_4(H_g)$	775.0 ⁱ	$\nu_3(H_u)$	606.0 ^b
$\nu_5(H_g)$	1101.0 ⁱ	$\nu_4(H_u)$	891.0
$\nu_6(H_g)$	1251.0	$\nu_5(H_u)$	1117.0 ^{b,i}
$\nu_7(H_g)$	1426.5	$\nu_6(H_u)$	1385.0
$\nu_8(H_g)$	1577.5	$\nu_7(H_u)$	1559.0 ^b

been refined here to optimize the overall agreement between the experimental values obtained from both the second-order ir and Raman⁸ spectra and the anticipated ($\nu_i + \nu_j$) values. Listed in Table II are the observed and

calculated ir mode frequencies obtained from this work and previous studies. In a few cases, more than one predicted combination mode frequency falls within $\pm 5 cm^{-1}$ (but most of them are within $\pm 2 cm^{-1}$) of the frequency of a particular higher-order ir feature. In such cases, the ir frequency determined experimentally is repeated in the table and assigned to more than one combination mode (see Table II). Overall, the difference between the calculated and observed frequencies is $\pm 4 cm^{-1}$, with very few exceptions. Of course, it is possible that some of the observed lines with frequencies $\nu \gg 2H_g(1)$ ($= 2 \times 272 cm^{-1}$) might be associated with third- and higher-order processes. Finally, it should be mentioned that some of the observed lines in Table II may be shifted slightly in frequency due to a Fermi resonance, a phenomenon in which a fundamental mode resonates with a combination mode. This effect is not included in our analysis.

Since the natural abundance of ^{13}C is approximately 1.1%, 34.4% of the molecules in our film should be monosubstituted $^{13}C^{12}C_{59}$ molecules (i.e., each of these molecules contains one ^{13}C and 59 ^{12}C atoms and 11.4% of the molecules should be $^{13}C_2^{12}C_{58}$). The lower symmetry (C_{2h}) of the monosubstituted $^{13}C^{12}C_{59}$ molecule is expected to activate all ir-silent modes that would otherwise be inactive in isotopically pure C_{60} , as previously observed, for example, in the vibrational spectra of benzene.¹³ In fact, our ir spectrum exhibits some weak lines whose frequencies are found to be in good agreement with certain fundamental mode frequencies: $H_g(3)$, $G_u(2)$, $H_g(4)$, $H_g(5)$, $H_u(5)$, $A_u(1)$, $A_g(2)$, and $G_g(6)$; these modes are therefore assigned to isotopically activated modes and they are identified by the superscript "i" in Tables I and II. However, not all of these fundamental mode frequencies have been uniquely determined. For instance, the lines assigned as $H_g(4)$, $H_u(5)$, and $A_g(2)$ in Table II can also be identified alternatively with the second-order combination modes " $H_g(2) + H_u(1)$," " $F_{2u}(2) + H_g(2)$ " [or " $H_g(4) + H_u(1)$ "], and " $G_u(2) + H_g(3)$ " [or " $H_g(4) + H_u(3)$ "], respectively, with comparable accuracy (see Table II). As expected, the frequency shift due to the monosubstitution of ^{13}C isotopes is found to be small (less than $2 cm^{-1}$, in most cases). Isotopic activation of silent C_{60} modes was also reported

TABLE II. Symmetry assignments for experimental ir lines observed in the transmission spectrum of C_{60} films deposited on KBr substrates. The labels "s" and "w" indicate, respectively, shoulders and weak features in the observed spectrum. As in Table I, the superscript "i" denotes ^{13}C isotope-activated modes.

Identification	Model	Expt	Identification	Model	Expt
$F_{1u}(1)$	526.5	526.5	$H_u(1) + G_g(1)$	828.5	822.9
$F_{1u}(2)$	575.8	575.8	$F_{2g}(1) + H_u(1)$	909	907.8 _w
		641.7 _w	$F_{2u}(2) + H_g(1)$	953	956.9 _s
$G_u(1) + H_g(1)$	672.5	673.5	$F_{1u}(1) + H_g(2)$	959	956.9 _s
$H_g(3)$	711.0 ⁱ	712.1	$H_u(1) + G_g(2)$	963.5	961.7
		738.1	$F_{2g}(1) + G_u(1)$	966	961.7
$G_u(2)$	760.0 ⁱ	757.4 _w	$G_g(2) + G_u(1)$	1020.5	1015.7
		770.9 _s	$G_u(2) + H_g(1)$	1033	1036.9
$H_g(4)$	775.0 ⁱ	774.7	$H_g(3) + H_u(1)$	1053.5	1058.1 _w
$H_g(2) + H_u(1)$	775	774.7	$H_g(5)$	1101.0 ⁱ	1099.6
$F_{1u}(1) + H_g(1)$	799	808.5 _w	$F_{2u}(2) + H_g(2)$	1112.5	1114.0

TABLE II. (Continued).

Identification	Model	Expt	Identification	Model	Expt
$H_u(5)$	1117.0 ⁱ	1114.0	$G_g(4)+H_u(4)$	1876.5	1874.5
$H_g(4)+H_u(1)$	1117.5	1114.0	$F_{2g}(1)+G_u(5)$	1876.5	1874.5
$A_u(1)$	1143.0 ⁱ	1141.0	$F_{1g}(1)+H_u(6)$	1887	1890.9
$F_{2u}(1)+G_g(3)$	1161.5	1164.1	$H_g(4)+H_u(5)$	1892	1890.9
$F_{2u}(2)+G_g(1)$	1166	1164.1	$F_{2u}(4)+H_g(3)$	1912	1912.1 w
$F_{1u}(3)$	1182.9	1182.9	$F_{1g}(1)+F_{1u}(4)$	1931.2	1934.3
$G_u(3)+H_g(1)$	1197	1196.9	$F_{1g}(3)+F_{1u}(2)$	1933.3	1934.3
$F_{1g}(1)+H_u(3)$	1198	1196.9	$F_{1u}(3)+H_g(4)$	1957.9	1957.4 w
$G_g(3)+G_u(1)$	1205.5	1203.7	$F_{2u}(4)+H_g(4)$	1976	1976.7
$F_{2g}(2)+H_u(1)$	1207.5	1213.3	$G_u(1)+H_g(8)$	1977	1976.7
$H_g(2)+H_u(4)$	1233.5	1234.5	$H_g(7)+H_u(2)$	1989.5	1988.3
$F_{1u}(1)+H_g(3)$	1237.5	1234.5	$H_g(2)+H_u(7)$	1991.5	1994.1 w
$G_u(4)+H_g(1)$	1243	1242.2	$A_g(2)+F_{1u}(1)$	1996.5	1994.1 w
$G_g(1)+G_u(2)$	1246	1242.2	$F_{2g}(1)+G_u(6)$	2012.5	2016.2 s
$F_{2g}(3)+H_u(1)$	1256.5	1258.6	$G_u(5)+H_g(3)$	2021	2023.9
$F_{1u}(2)+H_g(3)$	1286.8	1289.4	$G_u(3)+H_g(5)$	2025	2023.9
$G_g(1)+H_u(4)$	1287	1289.4	$G_u(4)+H_g(5)$	2071	2075.0
$F_{1g}(1)+H_u(4)$	1303	1306.8	$G_u(5)+H_g(4)$	2085	2083.7
$F_{2g}(1)+G_u(2)$	1326.5	1329.9 w	$H_g(3)+H_u(6)$	2096	2097.2
$H_g(4)+H_u(2)$	1338	1342.5	$F_{2u}(3)+G_g(4)$	2101.5	2097.2
$G_g(3)+H_u(2)$	1369	1375.2 w	$F_{2g}(4)+G_u(2)$	2120	2120.3
$G_g(2)+G_u(2)$	1381	1375.2 w	$F_{2u}(3)+H_g(5)$	2127	2131.4 s
$F_{1u}(4)$	1429.2	1429.2	$F_{1u}(4)+H_g(3)$	2140.2	2134.8
$H_g(5)+H_u(1)$	1443.5	1438.9 s	$F_{2g}(4)+H_u(4)$	2161	2163.7
$F_{2u}(3)+H_g(2)$	1458.5	1462.0 s	$F_{2g}(2)+G_u(5)$	2175	2174.3
$A_g(2)$	1470.0 ⁱ	1468.7	$G_u(3)+H_g(6)$	2175	2174.3
$G_u(2)+H_g(3)$	1471	1468.7	$G_u(2)+H_g(7)$	2186.5	2189.7
$H_g(4)+H_u(3)$	1471	1468.7	$G_g(3)+H_u(6)$	2191	2189.7
$F_{2g}(3)+H_u(2)$	1477	1479.3 s	$F_{1u}(4)+H_g(4)$	2204.2	2202.2 s
$F_{2u}(2)+G_g(3)$	1486	1483.2	$H_g(7)+H_u(4)$	2227.5	2234.1
$F_{2g}(1)+G_u(3)$	1490.5	1495.7	$H_g(3)+H_u(7)$	2270	2271.7
$G_u(1)+H_g(5)$	1500.5	1495.7	$H_g(8)+H_u(3)$	2273.5	2271.7
$G_g(3)+H_u(3)$	1502	1501.5	$F_{2u}(5)+H_g(3)$	2287.5	2290.0
$F_{1g}(2)+F_{1u}(1)$	1502	1501.5	$F_{2u}(4)+H_g(5)$	2302	2303.8
		1508.2 w	$G_g(5)+G_u(4)$	2326	2326.6
$F_{2u}(3)+G_g(1)$	1512	1514.0 w	$G_u(3)+H_g(7)$	2350.5	2346.8
$H_g(3)+H_u(4)$	1512	1514.0 w	$G_g(4)+G_u(5)$	2385.5	2388.3
$G_g(6)$	1524.5 ⁱ	1523.7 w	$G_u(5)+H_g(5)$	2411	2417.2
$G_u(2)+H_g(4)$	1535	1531.4 s	$F_{2u}(3)+H_g(7)$	2452.5	2456.7
$F_{1g}(2)+H_u(2)$	1538.5	1538.1	$G_g(4)+H_u(6)$	2460.5	2456.7
$G_g(2)+G_u(3)$	1545	1545.8 s	$F_{1u}(4)+H_g(5)$	2530.2	2527.1
$G_g(3)+G_u(2)$	1566	1570.9	$F_{2u}(4)+G_g(5)$	2557	2558.9
$H_g(4)+H_u(4)$	1576	1570.9	$F_{2u}(5)+H_g(5)$	2677.5	2675.5
$3F_{1u}(1)$	1579.5		$F_{1u}(4)+H_g(6)$	2680.2	2684.2 s
$F_{2u}(1)+H_g(6)$	1606.5	1607.5	$F_{2u}(4)+G_g(6)$	2725.5	2726.6 s
$G_g(3)+H_u(4)$	1607	1607.5	$G_u(5)+H_g(7)$	2736.5	2735.3
$3F_{1u}(2)$	1727.4		$F_{2u}(4)+H_g(8)$	2778.5	2772.9 w
$G_u(4)+H_g(4)$	1745	1746.3	$H_g(7)+H_u(6)$	2811.5	2809.5
$F_{1u}(1)+H_g(6)$	1777.5	1779.1	$G_g(6)+G_u(5)$	2834.5	2836.5
$F_{2u}(2)+H_g(5)$	1781	1779.1	$F_{1u}(4)+H_g(7)$	2855.7	2845.2
$F_{2g}(2)+G_u(3)$	1789	1789.7 w	$G_u(5)+H_g(8)$	2887.5	2884.7 w
$F_{2u}(3)+H_g(4)$	1801	1806.1 w	$A_g(2)+F_{1u}(4)$	2899.2	2894.3 w
$H_g(6)+H_u(2)$	1814	1815.7	$G_g(6)+H_u(6)$	2909.5	2908.8
$H_g(2)+H_u(6)$	1817.5	1815.7	$F_{1g}(3)+H_u(7)$	2916.5	2916.5 s
$F_{1u}(2)+H_g(6)$	1826.8	1824.4 w			2945.4 w
$F_{2g}(3)+G_u(3)$	1838	1841.8 w	$F_{2u}(5)+H_g(7)$	3003	2997.5
$F_{2u}(5)+H_g(1)$	1849.5	1851.4	$3F_{1u}(3)$	3548.7	
$G_g(1)+H_u(6)$	1871	1874.5	$3F_{1u}(4)$	4287.6	

recently in the Raman spectrum of solid C_{60} films.⁸

In analogy with observations of the higher-order Raman spectrum, one might expect that the strongest second-order vibrations would involve one of the four F_{1u} modes. Then by group theory, the most intense second-order ir lines should arise from the direct product $4F_{1u} \otimes n_j \Gamma_j$. This assumption implies that strong ir combination modes should occur for Γ_j equal to either A_g , F_{1g} , or H_g , which gives rise to a total of 52 combination modes. However, as can be seen in Table II, only nine of these combination modes are observed. Furthermore, as many as 41 combination modes that do not involve the F_{1u} modes are observed with appreciable intensity. It is interesting to note that: (i) of these 41 modes, 16 come from combinations of modes with F_{2g} , G_g , and H_u symmetries, all of which are otherwise silent in the first-order ir and Raman spectra, and (ii) 25 of these 41 combination modes involve the H_g modes which are Raman active in the first-order spectrum. Thus it appears experimentally that there is no simple rule (such as an F_{1u} mode should be involved in a strong higher-order ir line) to explain the oscillator strength of the individual second-order lines.

It should also be noted that many second-order combination modes predicted by group theory are omitted from Table II when a nearby feature is not observed experimentally. On the other hand, very few of the frequencies observed experimentally could not be associated

with either a second-order ir combination mode or an isotopically activated silent mode. The difficulty in making assignments to particular combination modes can be due to any one (or more) of the following reasons: (i) the anharmonicity responsible for activating the respective combination mode may induce a sizable shift in the mode frequency over that predicted by the sum of the fundamental frequencies of the participating modes; (ii) some of the observed frequencies may be due to third- or higher-order processes, i.e., although the second-order features are generally expected to be more intense, this need not be always the case; and (iii) some of the observed frequencies may be associated with difference modes ($\nu_i - \nu_j$) instead of sum modes ($\nu_i + \nu_j$).

Finally, it should be mentioned that it is very doubtful that the ir features assigned to the silent intramolecular modes are activated by crystal-field interactions, since at $T=300$ K the C_{60} molecules are known to be spinning very rapidly about their fcc lattice sites.¹⁴⁻¹⁶

The authors are grateful to Dr. P. Zhou and Professor G. W. Lehman for helpful discussions. This work was made possible by the financial support from the Center for Applied Energy Research (University of Kentucky) and NSF Grant No. ERR-91-08764. Research at MIT was funded by NSF Grant No. DMR-92-01878.

¹P. C. Eklund *et al.*, J. Phys. Chem. Solids **53**, 1391 (1992).

²D. S. Bethune *et al.*, Chem. Phys. Lett. **179**, 181 (1991).

³G. Dresselhaus, M. S. Dresselhaus, and P. C. Eklund, Phys. Rev. B **45**, 6923 (1992).

⁴W. Krätschmer, L. D. Lamb, K. Fostiropoulos, and D. R. Huffman, Nature **347**, 354 (1990).

⁵A. Lucas *et al.*, Phys. Rev. B **45**, 13 694 (1992).

⁶M. K. Nissen, S. M. Wilson, and M. L. W. Thewalt, Phys. Rev. Lett. **69**, 2423 (1992).

⁷C. Coulombeau *et al.*, J. Phys. Chem. **96**, 22 (1992).

⁸Z.-H. Dong *et al.*, Phys. Rev. B **48**, 2862 (1993).

⁹P. H. M. van Loosdrecht, P. J. M. van Bentum, M. A.

Verheijen, and G. Meijer, Chem. Phys. Lett. **198**, 587 (1992).

¹⁰B. Chase, N. A. Herron, and E. Holler, J. Phys. Chem. **96**, 4262 (1992).

¹¹A. M. Rao *et al.* (unpublished).

¹²A. F. Hebard, R. C. Haddon, R. M. Fleming, and A. R. Kortan, Appl. Phys. Lett. **59**, 2109 (1991).

¹³P. C. Painter and J. L. Koenig, Spectrochim. Acta **33A**, 1003 (1977).

¹⁴R. Tycko *et al.*, Science **253**, 701 (1991).

¹⁵P. A. Heiney *et al.*, Phys. Rev. Lett. **66**, 2911 (1991).

¹⁶W. I. F. David *et al.*, Europhys. Lett. **18**, 219 (1992).